AGU PUBLICATIONS

Tectonics

RESEARCH ARTICLE
10.1002/2013TC003461

Key Points:
- The Central Andes of NW Argentina acquired their modern elevation by 14 to 10 Ma
- Uplift was coupled with shortening and crustal thickening
- Lithospheric removal was small and did not affect elevation in the region

Supporting Information:
- Readme
- Figure S1
- Table S1
- Table S2
- Table S3
- Table S4

Correspondence to:
B. Carrapa,
bcarrapa@email.arizona.edu

Citation:
Carrapa, B., K. W. Huntington, M. Clementz, J. Quade, S. Bywater-Reyes, L. M. Schoenbohm, and R. R. Canavan (2014), Uplift of the Central Andes of NW Argentina associated with upper crustal shortening, revealed by multiproxy isotopic analyses, *Tectonics*, *33*, doi:10.1002/2013TC003461.

Received 9 OCT 2013
Accepted 16 MAY 2014
Accepted article online 22 MAY 2014

Uplift of the Central Andes of NW Argentina associated with upper crustal shortening, revealed by multiproxy isotopic analyses

Barbara Carrapa[1], Katharine W. Huntington[2], Mark Clementz[3], Jay Quade[1], Sharon Bywater-Reyes[3,4], Lindsay M. Schoenbohm[5], and Robin R. Canavan[3,6]

[1]Department of Geosciences, University of Arizona, Tucson, Arizona, USA, [2]Department of Earth and Space Sciences, University of Washington, Seattle, Washington, USA, [3]Department of Geology and Geophysics, University of Wyoming, Laramie, Wyoming, USA, [4]Now at Department of Geosciences, University of Montana, Missoula, Montana, USA, [5]Department of Chemical and Physical Sciences, University of Toronto, Mississauga, Mississauga, Ontario, Canada, [6]Now at Department of Geology and Geophysics, Yale University, New Haven, Connecticut, USA

Abstract This study contributes to the uplift history of the Andes, which has received increasing attention in recent years because of its implications for geodynamic models and climate feedbacks. Shortening resulting in crustal thickening and removal of gravitationally unstable mantle lithosphere has been proposed to control deformation and uplift of Cordillera-type orogenic systems such as the Puna Plateau of the central Andes and its eastern margin, the Eastern Cordillera. We present new clumped isotope (Δ_{47}), $\delta^{18}O$, and $\delta^{2}H$ data from carbonate nodules, marlstone, spring deposits, and volcanic ashes from the Puna Plateau and Eastern Cordillera of NW Argentina. When combined with other geological evidence, our data indicate that the Puna Plateau was near its present elevation since at least ~10 Ma, whereas the Eastern Cordillera rose ~1.5 km between ~14 and ~7 Ma. This history of uplift correlates with active shortening in the Eastern Cordillera and with incorporation of a regional foreland into the propagating orogenic wedge. Our study suggests that the elevation of the Puna Plateau changed little during the Miocene-Pliocene, whereas the margin experienced significant uplift associated with active deformation and crustal thickening.

1. Introduction

The Andes is a Cordillera-type orogenic system in which subduction of the oceanic Nazca plate under the continental South American plate has controlled a variety of processes such as magmatism, lithospheric removal, subduction, erosion and accretion, and shortening and crustal thickening [e.g., *Kley and Monaldi*, 1998; *Haschke et al.*, 2002; *Melnick and Echtler*, 2006]. The uplift history of the Central Andean Plateau, which includes the Altiplano Plateau of Bolivia and the Puna Plateau in northwest Argentina, has been linked both to crustal thickening [*Allmendinger et al.*, 1997] and more recently to isostatic rebound following lithospheric removal [*Molnar and Garzione*, 2007; *Garzione et al.*, 2006, 2008; *Leier et al.*, 2013]. A cyclical relationship between lithosphere removal, magmatism, deformation, and surface uplift has been proposed to govern Cordillera-type orogenic systems [*DeCelles et al.*, 2009]. According to this model, melt-fertile lower crust and upper mantle is underthrust beneath the arc, initiating melting and fractionation, which forms a dense (eclogitic) root. The excess of dense material beneath the arc decreases the rate of underthrusting, produces a regional isostatic depression of surface elevation within the plateau interior, and causes internal deformation and duplexing in the forearc region and in the retroarc wedge. When the arc root reaches critical mass, it is removed via a series of convective instabilities. Following root removal, regional uplift initiates outward propagation of the flanking orogenic wedges, upper crustal extension, and igneous flare-up. The cycle then begins again, with renewed underthrusting. In this model, shortening and crustal thickening are the key preconditions to initiate lithospheric instabilities and removal. The model thus makes useful predictions about what is required for lithospheric removal to happen; however, the expected magnitude of elevation changes during shortening and crustal thickening and following root removal remain largely unconstrained due to the uncertainties related to shortening estimates and volume of lithosphere removed.

Paleoaltimetry reconstructions suggest different uplift histories for different portions of the Central Andean Plateau, which includes the Altiplano of Bolivia and the Puna Plateau of Argentina, and for the Eastern

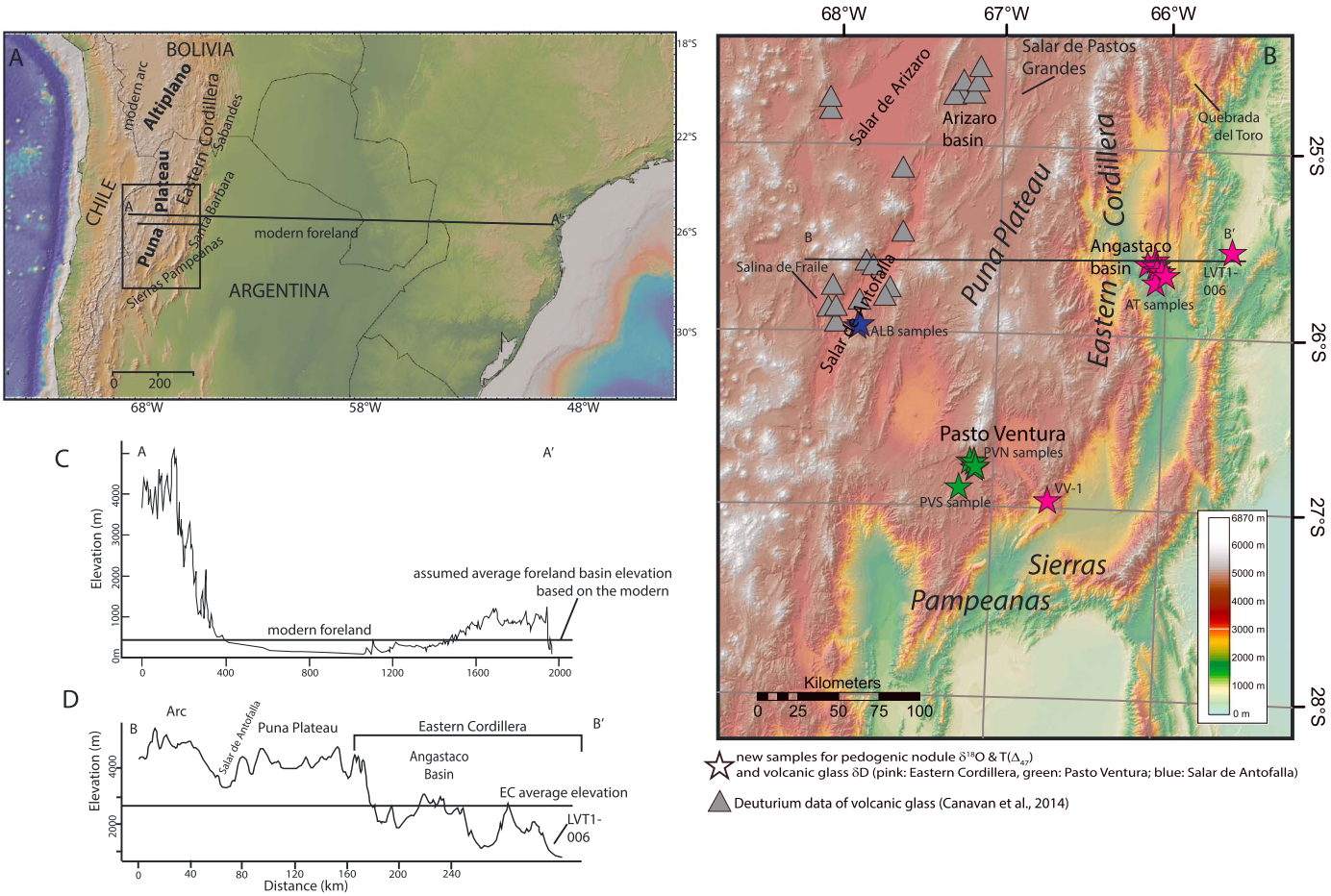

Figure 1. (a) Tectonomorphic map of the Central Andes, modified after *Carrapa et al.* [2011]; (b) digital elevation model of the study area with location of the analyzed samples; (c) swath profile across the Puna Plateau, Eastern Cordillera, and modern foreland of NW Argentina along A-A′ in Figure 1a; (d) B-B′ profile in Figure 1b.

Cordillera (Figure 1). Studies of the Altiplano have suggested significant Miocene uplift [e.g., *Gregory-Wodzicki*, 2000; *Ghosh et al.*, 2006a, 2006b; *Garzione et al.*, 2006, 2008; *Hoke and Garzione*, 2008; *Jordan et al.*, 2010]. In particular >2 km of uplift in the late Miocene in the Altiplano has been associated with wholesale delamination of mantle lithosphere beneath the plateau [*Molnar and Garzione*, 2007]. However, the timing and magnitude of uplift remain controversial [*Sempere et al.*, 2006; *Eiler et al.*, 2006; *Ehlers and Poulsen*, 2009; *Poulsen et al.*, 2010; *Insel et al.*, 2012]. *Garzione et al.* [2014] suggest that uplift of the Altiplano was asynchronous, with uplift of the southern portion of the Altiplano preceding uplift of the north central Altiplano by 7 ± 3 Ma. Another recent study suggests an older (25–15 Ma) episode of surface uplift of the Eastern Cordillera of Bolivia [*Leier et al.*, 2013], which the authors associate with lithospheric removal rather than with crustal shortening. Studies from the Puna Plateau to the south instead indicate a different history of protracted high elevation since the late Eocene [*Canavan*, 2010; *Canavan et al.*, 2014]. Therefore, no consensus exists on the uplift history of the Central Andean Plateau and of its eastern margin and on the underlying mechanism for the development and support of high topography. In particular, it is unclear if uplift is mainly the result of isostatic adjustments related to crustal thickening or removal of a dense layer of the lithosphere. Whereas several paleoaltimetry studies have been conducted on the Altiplano and Eastern Cordillera of Bolivia, only a few recent studies are available for the Puna Plateau of NW Argentina [*Canavan et al.*, 2014], no paleoaltimetry data exist for the Eastern Cordillera of NW Argentina, and no systematic study using multiproxy isotopic analysis is available for this part of the Andes.

This study presents the first carbonate Δ_{47} data for the Eastern Cordillera and Puna Plateau of NW Argentina (Figure 1). This, together with new δ^2H values of volcanic ashes and δ^{18}O values of carbonates, records the isotopic composition of meteoric water and local environmental temperatures, thus

constraining the paleoenvironmental and paleoelevation history of the region and testing current geodynamic models.

The wealth of data available for the Puna Plateau and for the Eastern Cordillera of NW Argentina makes it an ideal location to test the link between processes such as deformation, lithospheric removal, and surface uplift. We here concentrate on the Miocene to modern record because of the abundance of ashes and pedogenic carbonate nodules available for this time frame. We note that no ashes older than 14 Ma have been reported in the Eastern Cordillera of NW Argentina. For a discussion of the early Cenozoic uplift history of the Puna Plateau we refer to *Canavan et al.* [2014]. We hypothesize that deformation and uplift of the Eastern Cordillera of NW Argentina are controlled by shortening and crustal thickening. Our data, when combined with existing geological evidence, indicate that the elevation of the Puna Plateau changed little over the last 10 Ma, whereas the Eastern Cordillera experienced significant uplift (~1.5 km) between ~14 and 7 Ma, concomitant with wedge-top deposition. Our study argues for a coupling between shortening, crustal thickening, and uplift, whereas no direct link with lithospheric removal is observed.

2. Geological Background

What is now the Puna Plateau of NW Argentina was the site in the early Cenozoic of a regional retroarc foreland basin system [*DeCelles et al.*, 2011]. The orogenic front was at the location of the eastern Puna Plateau (Salar de Pastos Grande) by ~38 Ma [*Carrapa and DeCelles*, 2008] and was in the Eastern Cordillera by ~21 Ma [*Coutand et al*., 2001, 2006; *Carrapa et al*., 2011, 2012] (Figure 1). In particular the Angastaco basin, within the Eastern Cordillera and flanking the eastern margin of the Puna Plateau, was the site of a proximal foredeep between ~38 and 21 Ma—suggesting that the basin was at an elevation near or lower than ~400 m at this time (based on the modern Andean foreland basin elevation near the study area; Figure 1c). By ~14 Ma, the Angastaco basin was on top of the orogenic wedge and deforming internally [*Carrapa et al.*, 2012], as indicated by wedge-top deposits and the presence of an intraformational unconformity in ~14 Ma sedimentary strata [*Carrapa et al.*, 2011]. Deformation continued in the area until at least ~9 Ma, as indicated by growth structures in 11–9 Ma sedimentary rocks in the Quebrada del Toro (Figure 1) [*DeCelles et al.*, 2011], and propagated out of the Eastern Cordillera of NW Argentina after ~4 Ma [*Bywater-Reyes et al.*, 2010; *Carrapa et al.*, 2011]. Shortening estimates for the Eastern Cordillera are in the range of ~14–26% and suggests that most of the shortening occurred in the Miocene [*Grier et al.*, 1991; *Cristallini et al.*, 1997, 2004; *Kley and Monaldi*, 1998; *Mon and Salfity*, 1995].

Whereas much is known about the history of deformation, exhumation, and sedimentary basin evolution in the region [e.g., *Starck and Anzotegui*, 2001; *Coutand et al.*, 2001, 2006; *Deeken et al.*, 2006; *DeCelles et al.*, 2011; *Carrapa et al.*, 2012], limited data exist on its elevation history. Recent paleoelevation estimates indicate that the Puna Plateau was near its modern elevation as early as ~36 Ma [*Canavan et al.*, 2014]. This, together with other evidence indicating that the deformation front was located to the east of the modern Puna Plateau by ~38 Ma [*Carrapa and DeCelles*, 2008], implies significant crustal thickness under the Puna Plateau by late Eocene-Oligocene time. Previous workers proposed that the Puna Plateau was high and dry by as early as ~25 Ma based on the presence of extensive evaporite deposits within the plateau [*Vandervoort et al.*, 1995]. Gypsiferous deposits are found in the upper Eocene Quinõas Formation (~37 Ma) in Salina del Fraile [*Kraemer et al.*, 1999; *Carrapa et al.*, 2005] (Figure 1) indicating that aridity was established as early as 37 Ma. Limited erosion of the Puna Plateau since at least 25 Ma [*Carrapa et al.*, 2005, 2009; *Alonso et al.*, 2007; *Strecker et al.*, 2007; *Carrapa and DeCelles*, 2008] is consistent with sustained aridity, high elevation, and low internal relief since the early Miocene.

In order to investigate the uplift history of the Puna Plateau and in particular of the Eastern Cordillera and their relationships with deformation and upper crustal shortening, we analyzed the stable isotopic composition of carbonate and volcanic glass samples from the region. Samples of pedogenic carbonate nodules, lacustrine marls, spring deposits, and volcanic tuffs were collected within the Salar de Antofalla and Pasto Ventura (Puna Plateau) and within the Angastaco basin and surrounding areas (Eastern Cordillera) (Figure 1). Samples are restricted to the Miocene because of availability of suitable material for the isotopic analyses, which included hydrogen (δ^2H or δD), oxygen (δ^{18}O), and clumped isotope thermometry (Δ_{47}) methods.

3. Stable Isotope-Based Paleoaltimetry Approach

Conventional methods for reconstructing elevation histories from stable isotope data archived in minerals are based on the systematic decrease of the hydrogen (δ^2H or δD) and oxygen (δ^{18}O) isotopic values of meteoric water with increasing elevation, which occurs through the process of Rayleigh distillation as air masses rise to higher elevations [e.g., *Craig and Gordon*, 1965; *Dansgaard*, 1964; *Poage and Chamberlain*, 2001; *Blisniuk and Stern*, 2005; *Rowley and Garzione*, 2007]. Meteoric water O-isotopic compositions ($\delta^{18}O_w$) are then recorded by the δ^{18}O values of carbonate minerals ($\delta^{18}O_{cc}$) that precipitate from surface waters (e.g., carbonate formed from lake or soil water) and by the hydrogen isotopic composition of hydrated volcanic glasses (δ^2H_{glass}). Changes through time in the δ^2H and δ^{18}O values of meteoric water inferred from minerals can be used to reconstruct the elevation history of a region.

A number of complicating factors must be considered, including how well surface waters reflect meteoric water. Under most environmental conditions, δ^{18}O and δ^2H values for surface waters approach monthly averages for meteoric water. However, under arid conditions such as those that characterize the Puna Plateau today, δ^{18}O values for soil and surface waters can be enriched in ^{18}O by several per mil from local meteoric water values through evaporation [e.g., *Cerling*, 1984; *Cerling and Quade*, 1993; *Gazis and Feng*, 2004; *Hsieh et al.*, 1998; *Quade et al.*, 2007]. In contrast, hydration of volcanic glass is unaffected by evaporative enrichment. Meteoric water is absorbed by volcanic glass as it equilibrates to surface conditions, increasing the original water content of the glass (~0.2 wt %) to as much as 7–8 wt % and effectively overwriting the isotopic composition of inherent magmatic water [*Friedman et al.*, 1993]. This hydration process, which may require 10^3–10^4 years, creates a record of the hydrogen isotopic composition of past precipitation in the glass that is fixed and unaffected by further exchange with environmental waters [*Dettinger*, 2012; Quade, personal communication, 2014].

Since δ^2H values of surface waters are less affected by evaporative enrichment than are concomitant δ^{18}O values [*Craig and Gordon*, 1965], the δ^2H values of volcanic glasses are expected to provide a better estimate of the isotopic composition of meteoric waters—and therefore a more robust estimate of paleoenvironmental conditions and elevation—than δ^{18}O values of sedimentary carbonates, especially in extremely arid environments. In addition, in locations where carbonate and volcanic glass are both available for stable isotope analysis, an estimate for aridity can be obtained by calculating the offset in δ^{18}O water values determined from $\delta^{18}O_{cc}$ and δ^2H_{glass} values (converted to $\delta^{18}O_{water}$ values using the global meteoric water relationship: $\delta^{18}O_{water} = (\delta^2H_{water} - 10)/8$ [*Craig*, 1961]), which are differently affected by evaporation ($\Delta^{18}O_{cc\text{-}glass} = \delta^{18}O_{cc} - (\delta^2H_{glass} - 10)/8$). The magnitude of offset between these values positively correlates with the degree of aridity, such that larger offsets equate to more arid conditions. Differences between surface and meteoric waters in evaporative environments can thus be accounted for through our multiproxy approach.

The effect of seasonal variations in temperature on the isotopic composition of carbonates must also be considered. The δ^{18}O values of carbonate minerals are subject to the temperature-dependent isotopic fractionation between water and carbonate [e.g., *Cerling and Quade*, 1993; *Fan et al.*, 2011; *Fox and Koch*, 2004; *Liu et al.*, 1996], and thus the temperature of carbonate formation must be estimated in order to infer paleowater δ^{18}O values from carbonates. Soil and lake water temperatures generally vary predictably with air temperature [e.g., *Hillel*, 1982; *Hren and Sheldon*, 2012]. However, if carbonate forms seasonally, the temperature of carbonate formation may differ from mean annual soil or lake water temperatures [e.g., *Ghosh et al.*, 2006a; *Huntington et al.*, 2010]. In most settings, pedogenic carbonate formation is biased toward the warm season [*Breecker et al.*, 2009; *Snell et al.*, 2013; *Quade et al.*, 2007, 2011, 2013; *Passey et al.*, 2010; *Peters et al.*, 2013], although formation may occur under conditions closer to mean annual temperature in places with little seasonal temperature variation [*Passey et al.*, 2010] or in which the soils remain wet throughout the warm season [*Peters et al.*, 2013]. The temperature and timing of lacustrine carbonate formation is less well understood, but it is likely that biogenic and inorganic lake carbonate formation is also biased toward the warm season [*Huntington et al.*, 2010; *Quade et al.*, 2011]. To deal with this issue, we employ carbonate clumped isotope thermometry [*Ghosh et al.*, 2006b; *Eiler*, 2007, 2011] to provide a direct estimate of the temperature of carbonate formation ($T(\Delta_{47})$), constraining paleoenvironmental conditions and enabling the δ^{18}O values of water to be calculated from carbonate δ^{18}O values. Independent $T(\Delta_{47})$ estimates from clumped isotope thermometry both eliminate the need to assume the temperature of carbonate growth

to calculate paleowater $\delta^{18}O$ values from carbonate $\delta^{18}O$ values and provide independent estimates of paleoelevation based on the comparison of carbonate growth temperatures with surface temperature "lapse rates" or gradients in surface temperature with elevation [e.g., *Ghosh et al.*, 2006a; *Quade et al.*, 2007; *Huntington et al.*, 2010; *Lechler et al.*, 2013; *Leier et al.*, 2013].

Finally, the interpretation of paleoaltimetry data sets is complicated by the sensitivity of the isotopic composition of precipitation to the climatic conditions under which that precipitation is produced. Regional or global changes in temperature, humidity, wind direction (therefore source area), and amount of precipitation can all affect $\delta^{2}H$ and $\delta^{18}O$ values in precipitation [*Ehlers and Poulsen*, 2009; *Insel et al.*, 2012; *Leier et al.*, 2013; *Quade et al.*, 2007; *Rowley and Garzione*, 2007]. Since these conditions are not stable but may have varied over both short and long timescales in the Central Andes [e.g., *Vuille and Warner*, 2005], they can introduce considerable uncertainty into estimates of elevation based on $\delta^{18}O$ and $\delta^{2}H$ values from carbonates, volcanic glass, or other source materials. This is especially true for paleoelevation estimates based on modern isotopic lapse rates, which may be quite different from rates experienced for much of the Cenozoic Era. For the Andes, climate model simulations of seasonal environmental conditions have shown that isotopic lapse rates can change by up to 4.0‰ km^{-1} in response to temporal and spatial variations in temperature, elevation, and latitude [*Ehlers and Poulsen*, 2009; *Insel et al.*, 2012; *Sewall and Fricke*, 2013]. Also, studies of observations of O isotopes show seasonal and interannual variability of this same magnitude [*Vuille and Warner*, 2005]. Since our samples are restricted to the last 14 Ma, we avoid earlier time intervals (i.e., the Paleogene) when elevated atmospheric CO_2 concentrations would have caused global climate to have deviated sharply from present-day conditions in the Eastern Cordillera and Puna Plateau obfuscating elevation estimates [*Poulsen and Jeffery*, 2011].

Paleoaltimetry proxies are also affected by climate variability. Seasonality is indicated by the shifts in meteoric water $^{18}O/^{16}O$ ratios for pluvial times during the last glacial cycle [*Godfrey et al.*, 2003] and by modern land surface temperature data derived from Moderate resolution Imaging Spectroradiometer (MODIS) satellite data [*Wan et al.*, 2004] (supporting information Figure S1). Estimates of past climate variability from the Eastern Cordillera of NW Argentina suggest that temperatures varied by 3–4°C between Upper Pleistocene pluvial periods and the present day [*Bookhagen et al.*, 2001]. A similar degree of climate variability has been reported by *Godfrey et al.* [2003] based on the similarities and differences of meteoric $\delta^{18}O$ values from the Puna Plateau during Pleistocene pluvial times. Furthermore, erosion rates for the same time frame increased tenfold indicating significant environmental changes [*Bookhagen and Strecker*, 2012]. Thus, caution is still warranted, and correct interpretation of paleoaltimetry proxies requires a multiproxy approach.

We here combine standard methods of stable isotope paleoaltimetry with a novel application of $\delta^{2}H$ and $\delta^{18}O$ data to estimate aridity and with clumped isotope thermometry as an independent proxy for past temperature. These approaches allow us to evaluate changes in temperature, aridity, and $\delta^{18}O$ values of meteoric water as independent proxies for changes in elevation, reducing uncertainties in our estimates. This approach has limitations related to the fact that samples collected for $\delta^{18}O$ analyses may have formed at different times of the year and at different temperatures than the glass within the tuffs. This is particularly a problem for lacustrine samples due to high seasonal variability of $\delta^{18}O$ values in lake water [e.g., *Henderson and Shuman*, 2009]. However, the pedogenic carbonate nodules and tuffs collected for $\delta^{2}H$ and $\delta^{18}O$ analyses in this study mostly come from fluvial facies, which suggests similar paleoenvironmental conditions at the time of deposition.

Correct evaluation of paleotemperature and paleoelevation ultimately requires a combined analysis of isotopic data and other geological data. Our specific aim is to determine when environmental conditions similar to today were established on the Puna Plateau of NW Argentina (Pasto Ventura and Salar de Antofalla areas) and in adjacent areas along the margin of the Plateau in the Eastern Cordillera (the Angastaco basin and other locations). We use multiproxy paleoaltimetry data with independent geological information to determine the elevation history of the southern Puna Plateau and the Eastern Cordillera of NW Argentina.

4. Analytical Methods

4.1. Analysis of Volcanogenic Glasses

Volcanic glass was separated from tuffs from the Eastern Cordillera ($n = 9$; seven from the Angastaco basin, one from the Villavil (VV) section, and one from the La Viña/Allemania section; Figure 1b) and Puna Plateau

($n = 4$; three from the Pasto Ventura and one from the Salar de Antofalla regions) using methods modified from *Cassel et al.* [2009]. See supporting information (Table S1) for sample details. After disaggregating tuffs in a ceramic mortar and pestle, carbonate was removed by addition of 6 N HCl, followed by rinsing in Deionized (DI) water (3 times). Samples were then sieved to separate the 250–125 μm and 125–53 μm size fractions, the size fraction that ensures sufficient hydration without alteration to clay [*Friedman et al.*, 1993]. Glass from these fractions was separated by a combination of heavy liquid separation (lithium polytungstate, $\rho = 2.2$ to 2.25 g/mL), ultrasonication in DI water (to remove adhering clays), and passage through a Frantz Isodynamic Separator (to remove biotite). Purity of samples (~99% glass) was confirmed via visual inspection with a petrographic microscope.

Stable isotope analysis of glass samples (2–3 mg) was performed at the University of Arizona's Environmental Isotope Laboratory. Approximately 2–3 mg aliquots of glass were packed into silver foil and analyzed in triplicate on a thermal conversion elemental analyzer coupled with a Delta V plus isotope ratio mass spectrometer. Instrument precision (1 σ) was 2.5‰ based on repeated analysis of internal lab standards and international standard reference materials (PEF-1, NBS-22, and NBS-30). Stable isotope values are reported in per mil (‰) using delta (δ) notation [$\delta = (R_{sample}/R_{standard} - 1) \times 1000$] where R represents the respective isotope ratio ($^2H/^1H$) of sample and standard (Vienna standard mean ocean water (VSMOW)).

4.2. ^{18}O Analysis of Pedogenic Carbonate Nodules

Sedimentary carbonates intended for conventional ($\delta^{18}O$, $\delta^{13}C$) stable isotopic analyses were sectioned using a rock saw, and powder samples (~5 mg) were drilled from the micritic interior using a Dremel drill (0.6 mm bit). Care was taken to avoid contamination by secondary carbonates (spar). Three powder samples were collected from each carbonate sample unless small specimen size made this impractical. Powders were then weighed (100–200 μg) into glass vials, dried overnight (50°C), capped, and then flushed with He before reaction with 100% phosphoric acid (100 μL) for a minimum of 24 h. The CO_2 produced and concentrated in the headspace of the vial was then analyzed using a Thermo Finnigan GasBench II connected to a Thermo Finnigan Delta Plus XP continuous flow isotope ratio mass spectrometer at the Stable Isotope Facility at the University of Wyoming. Instrument precision (1 σ) was better than 0.1‰ for $\delta^{13}C$ values and 0.2‰ for $\delta^{18}O$ values based on repeated measure of internal lab standards and international standard reference materials (NBS18, NBS19). Stable isotope values are reported in per mil (‰) using delta (δ) notation [$\delta = (R_{sample}/R_{standard} - 1) \times 1000$] where R represents the respective isotope ratio ($^{13}C/^{12}C$, $^{18}O/^{16}O$) of sample and standard (Vienna Peedee belemnite (VPDB)).

4.3. Clumped Isotope Thermometry Analysis

A subset of the carbonate samples from the Angastaco basin (ranging in age from ~8 Ma to ~3 Ma; Table S3) and Puna Plateau (ranging in age from ~10 Ma to ~0.5 Ma; Table S3) were analyzed for clumped isotope thermometry (Δ_{47}, $\delta^{13}C$, and $\delta^{18}O_{cc}$) at the California Institute of Technology (CIT). Analyses were performed on two ThermoFinnigan MAT 253 mass spectrometers (MS-I and MS-II) configured to measure m/z 44–49 inclusive [*Eiler and Schauble*, 2004; *Affek et al.*, 2007]. The samples included 11 pedogenic calcite nodules from the Angastaco basin and calcite from three soil nodules and one lacustrine marlstone from the Pasto Ventura and Salar de Antofalla regions of the Puna Plateau (Table S3). For each of the 34 analyses of these samples, 8 to 9 mg of calcite was digested in anhydrous phosphoric acid under vacuum and purified cryogenically and using gas chromatography. The MS-I samples were digested at 25°C and purified using the methods of *Ghosh et al.* [2006a] and *Huntington et al.* [2010], and the MS-II samples were digested at 90°C and purified using the methods of *Passey et al.* [2010]. Following purification, the CO_2 was transferred to a mass spectrometer for isotopic ratio analysis. The in-house carbonate Δ_{47} standard Carrara marble was analyzed along with the samples (accepted Δ_{47} value 0.352‰ in the CIT reference frame—see below) and yielded an average value of 0.345 ± 0.010‰ for MS-I and 0.350 ± 0.009‰ for MS-II (1 standard deviation), showing good agreement between the two methodologies and mass spectrometers (Table S4).

The analyses were conducted prior to the creation of the absolute reference frame (carbon dioxide equilibrium scale) described by *Dennis et al.* [2011], so we report Δ_{47} data relative to the CIT intralab reference frame, which is normalized to analyses of CO_2 heated to 1000°C [*Huntington et al.*, 2009]. Heated gas and carbonate standard data are reported in the supporting information (Table S4). Analyses were screened for contaminants using mass 48 values [e.g., *Eiler and Schauble*, 2004; *Guo and Eiler*, 2007; *Huntington et al.*, 2009],

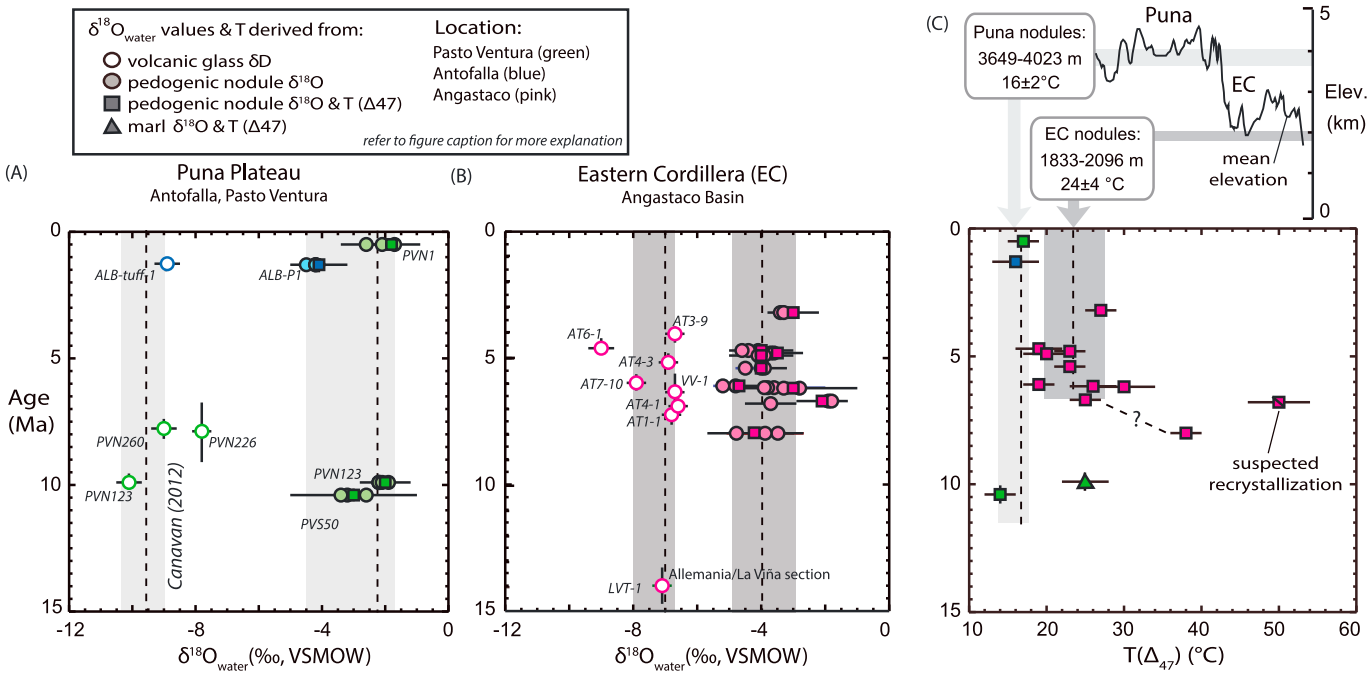

Figure 2. Stable isotopic data for Cenozoic volcanogenic glass and sedimentary carbonates from (a) the Puna Plateau and (b) the Eastern Cordillera. Vertical dashed lines represent median $\delta^{18}O$ values for meteoric water determined from volcanogenic glass and sedimentary carbonates with shaded areas defining the first quartile (25th percentile) and second quartile (75th percentile) for samples from the Puna Plateau (light gray; this study (sedimentary carbonates) and *Canavan et al.* [2014] (volcanogenic glass)) and Eastern Cordillera (dark gray). Meteoric water δ^2H values determined from volcanogenic glass were converted to $\delta^{18}O$ values using the Global Meteoric Water Line [*Craig and Gordon*, 1965]. Carbonate $\delta^{18}O$ values were converted to water $\delta^{18}O$ values using temperatures determined by clumped isotope (Δ_{47}) analysis (values plotted in °C) of a subset of pedogenic and marl carbonates from each sampling area. Error bars represent ± 1 SE. (c) Temperatures calculated based on Δ_{47} analyses presented in this study. Refer to text for explanation.

and results are reported only for samples with Δ_{48} values within 2‰ of the heated gas δ_{48} versus Δ_{48} line. For samples digested at 90°C, the reported Δ_{47} value includes an acid digestion correction of 0.081‰, which was determined empirically in the CIT lab using the same methods and during the same time period over which the samples were analyzed [*Passey et al.*, 2010]. The data are thus consistent with the initial calibration data of *Ghosh et al.* [2006a], and so we convert sample Δ_{47} values into carbonate growth temperature estimates ($T(\Delta_{47})$) using the *Ghosh et al.* [2006a] calibration, with errors propagated following *Huntington et al.* [2009]. For reference, Δ_{47} values estimated using a tertiary transfer function based on analyses of carbonate standards [*Dennis et al.*, 2011] are reported in the absolute reference frame in the supporting information (Tables S3 and S4), although these values are only approximate and are not considered in the discussion.

5. Stable Isotopic Results

5.1. Volcanic Glass δ^2H Results

Hydrogen isotopic values for glass samples (δ^2H_{glass}) from the Eastern Cordillera and from the Pasto Ventura and Salar de Antofalla regions in the Puna Plateau were compared with previously analyzed samples from the Puna Plateau (Arizaro basin and Salina del Fraile; *Canavan et al.* [2014]) (Figures 1 and 2). Our new Puna Plateau samples from Pasto Ventura and Salar de Antofalla (mean δ^2H_{glass} value = −94 ± 8‰, $n = 4$) yield similar values to other samples (Eocene to modern) from the Puna Plateau (mean δ^2H_{glass} value = −99 ± 11‰, $n = 10$ [*Canavan et al.*, 2014]). Samples from the Puna Plateau have consistently lower isotopic values (i.e., higher reconstructed elevations) than samples from the Eastern Cordillera (mean $\delta^2H_{glass} = -78 \pm 7$‰, $n = 9$) (Table S1). Using the fractionation factor between the δ^2H value of volcanic glass and of meteoric water (1.0343 [*Friedman et al.*, 1993]), corresponding δ^2H meteoric water values (δ^2H_{mw}) for the Puna Plateau and Eastern Cordillera samples are calculated to have been around −70‰ and −45‰, respectively.

We converted δ^2H_{mw} values determined from volcanic glass to meteoric water $\delta^{18}O$ values ($\delta^{18}O_{mw}$) using the global meteoric water relationship: $\delta^{18}O_{mw} = (\delta^2H_{mw} - 10)/8$ [*Craig*, 1961]. Calculated $\delta^{18}O_{mw}$ values show about a 2‰ offset between samples from the Puna Plateau (-9.0 ± 0.9‰) and Eastern Cordillera (-7.1 ± 0.8‰) (Figures 2a and 2b). In general no relationship between isotopic values and sample age is observed. In general, our $\delta^{18}O_{mw}$ values are comparable to the range of values reported by *Canavan et al.* [2014] for Eocene to modern ash deposits within the Puna Plateau. In the following section, these values are combined with $\delta^{18}O$ water values calculated from pedogenic carbonate nodules to compare the degree of aridity between the Puna Plateau and Eastern Cordillera.

We estimate paleoelevation of the samples using an empirically derived equation of $\delta^2H_{mw} = -13.7$‰ km^{-1} × elevation (in km) − 9.0 ($R^2 = 0.90$), relating elevations and δ^2H values of meteoric waters [*Dettinger*, 2012; Quade, personal communication, 2014]. Using this approach, elevations for the Eastern Cordillera are calculated to have been > 2.0 km since at least 7 Ma based on eight volcanic glass analyses from tuffs mostly within fluvial deposits of the Angastaco basin (Figure 1b) (samples, Table S1); modern average elevation of the Eastern Cordillera is ~2.7 km (Figure 2c). For sample LVT1-006 (Table S1), which is from a lacustrine bed from the La Viña section ~80 km east of Angastaco basin, the same equation suggests paleoelevations that are twice the modern elevation (Table S1). We interpret this high paleoelevation estimate to reflect the hypsometric mean elevation of the drainage basin [*Rowley and Garzione*, 2007; *Saylor et al.*, 2009] rather than the local elevation of the sample. Therefore, the high elevation recorded by sample LVT1-006 represents mean elevation of the Eastern Cordillera at ~14 Ma. Using the same equation for δ^2H_{mw} values from four samples from the Pasto Ventura and Salar de Antofalla, elevations for the Puna Plateau are calculated to have been > 3.0 km since ~10 Ma (Table S1).

5.2. Carbonate $\delta^{18}O$ and $\delta^{13}C$ Results

Isotopic results for carbonate samples from the Puna Plateau and Eastern Cordillera are presented in the supporting information (Table S2) and summarized here. Carbonate $\delta^{18}O$ (VPDB) values ($\delta^{18}O_{cc}$) for six pedogenic carbonate nodules (from fluvial deposits), a sample of lake marlstone, and two samples of spring deposits collected in Miocene-Pliocene deposits from the Puna Plateau region ranged from −4.9‰ to −2.4‰ with no apparent relationship with age, location, or carbonate type (Figure 2a).

The 32 pedogenic carbonate nodules collected from Miocene-Pliocene deposits of the Angastaco basin show $\delta^{18}O_{cc}$ (VPDB) values that range between −9.7‰ and −3.9‰ (Table S2). These data agree with previous results showing a shift from low (−9.7 to −7.9‰) to higher values (−6.9 to −3.9‰) between ~8 Ma and 5.5 Ma, which has been interpreted to represent a change from more humid climate conditions (>5 Ma) to sustained aridity at ~5.5 Ma [*Bywater-Reyes*, 2009]. This interpretation is also supported by $\delta^{13}C$ values determined from these carbonates (Table S2) [*Bywater-Reyes*, 2009] and from associated mammalian tooth enamel, which show a similar shift from low (−15.5 to −10.2‰ VPDB) to higher (−9.5 to −8.1‰ VPDB) values [*Bywater-Reyes*, 2009], suggesting that environmental conditions became drier.

6. Clumped Isotope Thermometry Results

The clumped isotope analyses (Table S3) provide independent estimates of calcite precipitation temperature, $\delta^{13}C$ and $\delta^{18}O_{cc}$ values, from which the $\delta^{18}O_w$ values of the parent waters can be calculated [*Ghosh et al.*, 2006a, 2006b; *Eiler*, 2007, 2011]. The nine youngest (6.2 to 3.2 Ma) Angastaco basin samples yielded plausible soil temperatures ranging from 19 to 30°C (average 24 ± 4°C, 1 σ). Using the fractionation factor of *Kim and O'Neil* [1997], calculated values of the $\delta^{18}O_w$ of the soil waters from which these samples precipitated range from −4.7 to −2.1‰ (mean −3.7 ± 0.7‰ VSMOW). The oldest (8.0 Ma) Angastaco sample yielded a warmer temperature of 38°C and a calculated $\delta^{18}O_w$ value of −4.2‰ (VSMOW) that is consistent with the other soil water values. These temperatures are in the range of $T(\Delta_{47})$ values observed for modern/Holocene pedogenic carbonates from the Andes and elsewhere and paleosol carbonates from the Altiplano and Subandes [e.g., *Quade et al.*, 2013; *Peters et al.*, 2013; *Garzione et al.*, 2014]. In contrast, the 6.3 Ma Angastaco sample yielded a significantly warmer temperature of 50°C and an anomalously high $\delta^{18}O_w$ value of 1.1‰, suggesting that the sample was diagenetically altered, as discussed below. Clumped isotope temperature estimates for pedogenic nodules from the Puna Plateau (10–0.5 Ma) range from 14 to 17°C and are indistinguishable within uncertainty (average 16 ± 2°C). The Puna Plateau marl sample (9.9 Ma) yielded a warmer $T(\Delta_{47})$ value of 25°C, but this

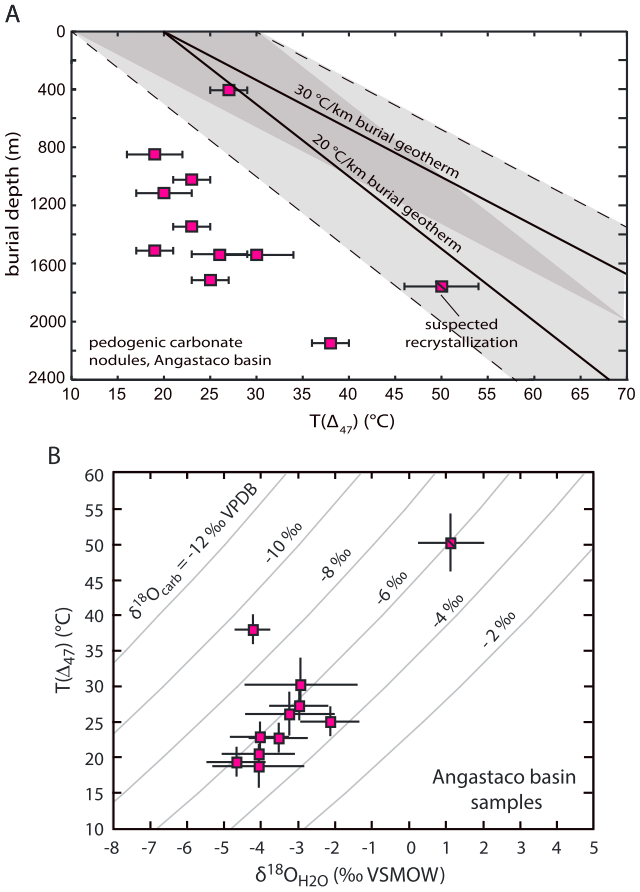

Figure 3. Measured $T(\Delta_{47})$ values for pedogenic carbonate nodules from the Angastaco basin (squares) plotted versus (a) estimated maximum burial depth and (b) apparent $\delta^{18}O_w$ values for the samples. In Figure 3a squares show sample temperatures with 1 SE error bars. For reference, the heavy solid lines show estimated burial geotherms, assuming a surface temperature of 20°C and a gradient of 30°C/km or 20°C/km. The shaded regions outlined by dashed lines indicate ±10°C offsets from these trends, which we consider a reasonable estimate of uncertainty. In Figure 3b sample $T(\Delta_{47})$ values were calculated using the calibration of *Ghosh et al.* [2006a, 2006b], and $\delta^{18}O_w$ values were calculated using the calcite-water oxygen isotope thermometry equation of *Kim and O'Neil* [1997] (as in Table S3). Squares are sample data with 1 SE error bars. Gray contours are solutions to the calcite-water oxygen isotope thermometry equations for constant $\delta^{18}O_{cc}$ values. If closed system reordering in a diagenetic environment with a high rock:water ratio is responsible for the elevated clumped isotope temperatures, $T(\Delta_{47})$ is expected to increase along contours of constant $\delta^{18}O_{cc}$ $^{18}O_{carb}$.

temperature estimate is not directly comparable to the soil nodule temperatures due to the lacustrine nature of the deposit. Estimates of the $\delta^{18}O$ values of the lake and soil waters in equilibrium with the Puna Plateau samples range from −4.1 to −1.8‰, similar to the range observed for the Angastaco basin samples (Figure 2).

The elevated temperature and $\delta^{18}O_w$ value of the 50°C Angastaco basin sample (6.3 Ma) suggest diagenetic alteration, which can occur either via recrystallization or by diffusive C—O bond reordering [see *Passey and Henkes*, 2012]. The Angastaco basin samples were only buried to ~2 km depth and heated to maximum burial temperatures of ~80° to 100°C (Figure 3), ruling out diffusive C—O bond reordering [*Henkes et al.*, 2014]. The 50°C sample temperature therefore reflects recrystallization conditions. The sample's $\delta^{18}O_{cc}$ value of −5.9‰ (VPDB) is similar to the $\delta^{18}O_{cc}$ values of the 19–30°C Angastaco basin samples, suggesting that recrystallization occurred in a closed-system, rock-buffered (i.e., high rock:water ratio) environment. Under such conditions, the sample $\delta^{18}O_{cc}$ value would remain approximately constant while the $\delta^{18}O_w$ value became enriched in ^{18}O and $T(\Delta_{47})$ increased. Figure 3b shows that this pattern is observed for the 50°C sample. As a consequence, neither the sample temperature nor the calculated $\delta^{18}O_w$ value provides useful paleoenvironmental information.

It is unlikely that this mechanism affected the 38°C (8 Ma) Angastaco basin sample. If the 38°C sample had originally recorded similar depositional conditions as the 19–30°C samples and been recrystallized in a rock-buffered environment, we would expect it to have an elevated $\delta^{18}O_w$ value and plot near the 4–6‰ (VPDB) $\delta^{18}O_{cc}$ contour in Figure 3b. But this sample's water $\delta^{18}O$ is consistent with that of the other samples, giving us no reason to suspect that the 38°C temperature does not represent primary environmental conditions.

The clumped isotope temperatures can be combined with conventional carbonate $\delta^{18}O_{cc}$ values and $\delta^{2}H$ values from glass to estimate paleowater $\delta^{18}O_w$ values, for comparison to the soil water $\delta^{18}O_w$ values given by the clumped isotope samples. We compared (1) soil water $\delta^{18}O_w$ (VSMOW) values calculated from carbonate $\delta^{18}O_{cc}$ values and formation temperatures with (2) volcanic glass-based estimates of $\delta^{18}O_w$ calculated by converting

estimates of meteoric water δ^2H values from glass to δ^{18}O values using the global meteoric water relationship: $\delta^{18}O_{water} = (\delta^2H_{water} - 10)/8$ [*Craig*, 1961]. Estimates for meteoric water δ^{18}O values for the Angastaco basin (mean $\delta^{18}O_{mw} = -7.1 \pm 0.8$‰ (VSMOW)), Pasto Ventura and Salar de Antofalla (mean $\delta^{18}O_{mw} = -9.0 \pm 0.9$‰), and northern Puna Plateau (mean $\delta^{18}O_{mw} = -10 \pm 1.7$‰ [*Canavan et al.*, 2014]) were significantly lower than soil water $\delta^{18}O_w$ values calculated from carbonates (Figures 2a and 2b).

The calculated offset ($\Delta^{18}O_{w\text{-}mw}$) between $\delta^{18}O_w$ values for soil (from carbonates) and $\delta^{18}O_{mw}$ for meteoric waters (from glass) from the Puna Plateau (Pasto Ventura and Salar de Antofalla; 6 ± 2‰; Figure 2a) is greater than that calculated for the Eastern Cordillera samples (ages 8.0 to 3.2 Ma; 3 ± 2‰; Figure 2b and Table S2).

7. Discussion

The establishment of environmental conditions similar to modern on the Puna Plateau since ~10 Ma, and as early as 36 Ma [*Canavan*, 2012; *Canavan et al.*, 2014], and in the Eastern Cordillera since 14 to 7 Ma is evident from examination of meteoric water δ^{18}O values determined from volcanic glass (δ^2H_{glass} $^2H_{glass}$) and carbonate materials ($\delta^{18}O_{cc}$) (Figures 2a and 2b). The ~6‰ difference between δ^{18}O values derived from volcanic glass (-9.0 ± 0.9‰) and δ^{18}O values derived from pedogenic carbonate nodules (-2.7 ± 0.9‰) indicates sustained aridity in the Puna Plateau since at least 10 Ma.

Conversion of meteoric water δ^2H values determined from volcanogenic glass to corresponding $\delta^{18}O_{mw}$ values produces lower values for the Puna Plateau (−9.0‰) than for the Eastern Cordillera (−7.1‰). These values agree with modern precipitation δ^{18}O values for both areas. In the Eastern Cordillera, δ^{18}O values for precipitation have been measured at three stations near our field sites in Argentina: Purmamarca, elevation 2400 m; Los Molinos, 1300 m; and Salta, 1187 m. Long-term weighted means for precipitation δ^{18}O values at these locations are −8.0‰, −6.3‰, and −6.5‰, respectively [*IAEA/WMO*, 2014], and are in good agreement with our calculation of a mean $\delta^{18}O_{mw}$ value of -7.1 ± 0.8‰ from our volcanic glass samples. Although direct measurements of precipitation from the Puna Plateau are not available, precipitation δ^{18}O values have been determined from stations at similar elevations in Chile (−9.8‰ to −10.2‰ [*IAEA/WMO*, 2014]), which are in close agreement with the mean $\delta^{18}O_{mw}$ for our four sites (-9.0 ± 0.9‰) and others from the northern Puna Plateau (-10 ± 1.7‰ [*Canavan et al.*, 2014]). In addition, our $\delta^{18}O_{mw}$ values for the Puna Plateau are similar to modern atmospheric water vapor δ^{18}O values obtained from Salar de Hombre Muerto region [*Godfrey et al.*, 2003]. The consistent difference in precipitation δ^{18}O values at these two locations today and in the past supports our interpretation suggesting that the present elevation difference between the Puna Plateau and Eastern Cordillera has been in place and by inference paleoenvironmental conditions similar to modern were acquired since at least 7 Ma.

In contrast, the difference in $\delta^{18}O_{cc}$ values at both sites is negligible, with $\delta^{18}O_w$ values derived from carbonates centering on −3 to −4‰ in the Puna Plateau and Eastern Cordillera (Figures 2a and 2b). The greater offset between $\delta^{18}O_w$ values determined from carbonates and $\delta^{18}O_{mw}$ values determined from volcanogenic glass for the Puna Plateau (6 ± 2‰) than for the Eastern Cordillera (3 ± 2‰) is consistent with the interpretation that while both areas experienced arid conditions, the Puna Plateau was significantly drier leading to greater evaporation of source waters than in the Eastern Cordillera since at least 10 Ma (Figures 2a and 2b).

Overall $\delta^{18}O_w$ values calculated from pedogenic carbonate nodules in the Puna Plateau are consistently higher than values recorded in the Altiplano of Bolivia [*Garzione et al.*, 2008; *Bershaw et al.*, 2010] and in the Eastern Cordillera of Argentina [*Bywater-Reyes et al.*, 2010] and are interpreted to record intense evaporation related to an arid environment established since at least the middle to late Miocene—consistent with the establishment of high elevation by this time (Figure 4). This interpretation is bolstered by the observations of extensive evaporites preserved in the Puna Plateau since ~36 Ma and Miocene eolian deposits in both the Puna and Eastern Cordillera [*Vandervoort et al.*, 1995; *Carrapa et al.*, 2009, 2011; *Starck and Anzotegui*, 2001; *DeCelles et al.*, 2011]. We suggest that $\delta^{18}O_{cc}$ variations in Puna Plateau carbonates do not represent true changes in elevation but rather changes in evaporation in response to increased aridity. The δ^2H_{glass} values from tuffs collected from the Puna Plateau and Eastern Cordillera are consistent with this interpretation, showing a marked difference in values between the Puna Plateau samples (lower values of ~ −99‰: higher

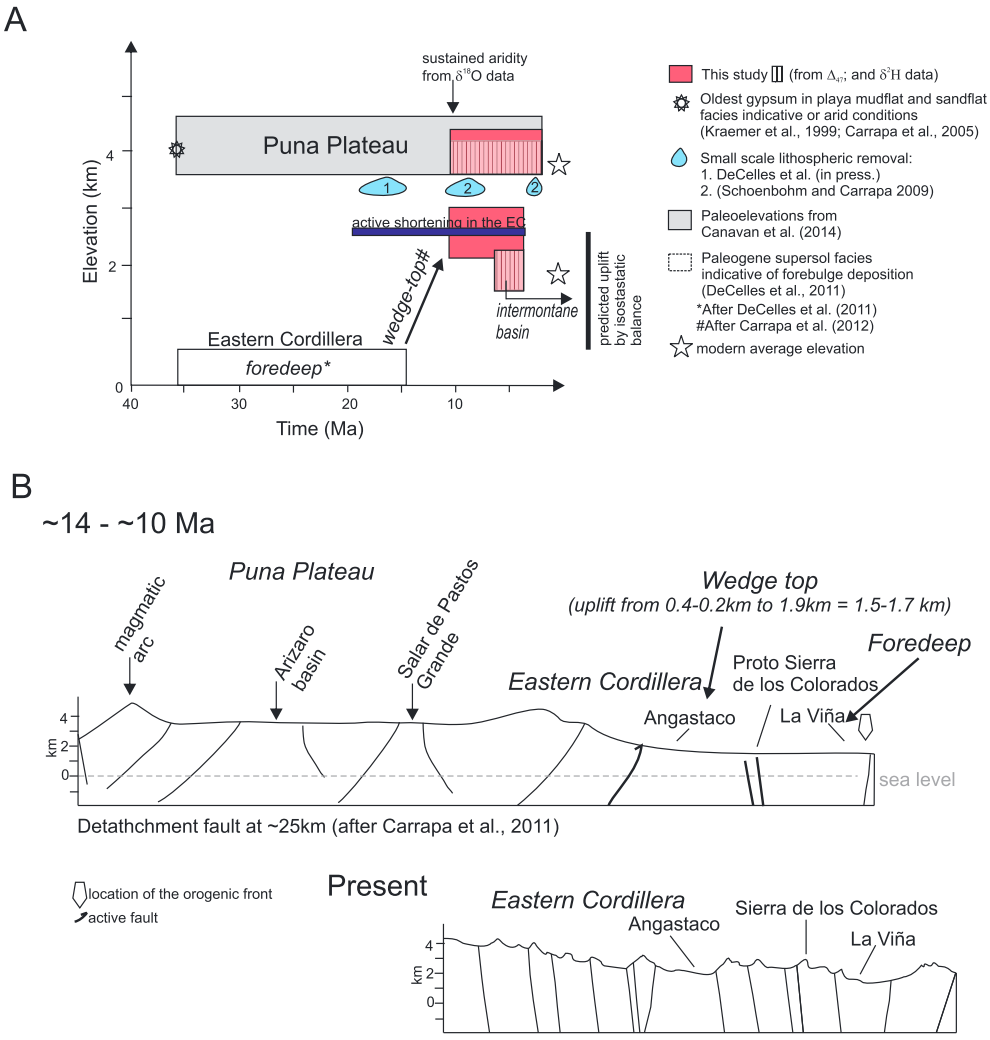

Figure 4. (a) Summary time-elevation diagram showing the elevation history of the Puna Plateau and Eastern Cordillera based on this study and other published work. Paleoelevation calculations from δ^2H values are presented in Table S1, and those from clumped data are explained in the text. (b) Schematic cross sections (vertically exaggerated) at different times for the Puna Plateau and Eastern Cordillera indicating the location of the foreland basin depozones and of the orogenic front. Uplift calculated assuming airy isostasy and area balance calculation; refer to text for more explanations. A 25% shortening, an initial undeformed length of the Eastern Cordillera of 275 km and a final shortened length of 205 km [*Grier et al.*, 1991], an original crustal thickness of 40 km (based on modern crustal thicknesses under the present foreland [*Beck and Zandt*, 2002]), and crust and mantle density of 2.8 and 3.3 g/cm^3, respectively.

elevation) and the Eastern Cordillera samples (higher values of ~ −78‰: lower elevation) since ~10 Ma (Figure 2b). Interesting modern deuterium values for the nearby Salar de Hombre Muerto waters are ~80 per mil suggesting that some areas of the Puna Plateau (e.g., Arizaro [*Canavan et al.*, 2014]) may have been higher than today in the Miocene.

In order to further evaluate changes in isotopic compositions as a function of temperature and elevation, we analyzed the differences in pedogenic calcite nodule $T(\Delta_{47})$ values recorded by different age samples within the Puna Plateau and Eastern Cordillera and compared these values to modern environmental temperatures for the region. Recent studies have shown that pedogenic carbonate formation is biased toward the warm season [*Breecker et al.*, 2009; *Passey et al.*, 2010; *Quade et al.*, 2007, 2011, 2013] except in cases where summer precipitation prevents soil drying out until fall, when soil temperatures are closer to mean annual temperature [*Peters et al.*, 2013]. Although the Puna Plateau receives summer precipitation, the summer rains are sufficiently infrequent that complete drying is likely to occur rapidly, resulting in soil

carbonate formation during the summer, despite it being the wet season. Thus, we consider soil nodule formation temperatures to approximate summer air temperatures in this region. Modern air temperature estimates (12 year average air temperature inferred from MODIS data (Figure S1)) indicate that for the Pasto Ventura area, modern mean annual air temperature (MAAT) is 8.6°C and summer (December-January-February (DJF)) air temperature is 15.8°C. This summer air temperature is indistinguishable from the average Puna Plateau nodule sample temperature of 16 ± 2°C. The Angastaco area MAAT is 22.2°C, and summer (DJF) air temperature is 27.3°C, within error of the average Angastaco paleosol nodule $T(\Delta_{47})$ value of 24 ± 4°C for the 6.2 to 3.2 Ma samples. The close correspondence of pedogenic calcite nodule $T(\Delta_{47})$ values and modern temperatures suggests that soil paleotemperatures in the Angastaco basin and Puna Plateau were not significantly different from modern temperatures over this interval. The 8 Ma Angastaco paleosol nodule yielded a higher temperature of 38°C, raising the intriguing possibility that the Angastaco basin was warmer, and potentially at lower elevation, at this time. The $\delta^{18}O_w$ value of the soil water from which the sample grew (−4.2‰ VSMOW) is consistent with the other Angastaco basin and Puna Plateau samples. However, because $\delta^{18}O_w$ values likely reflect aridity and/or precipitation amount [*Insel et al.*, 2013], we cannot use the 38°C sample's $\delta^{18}O_w$ value to test the hypothesis that the decrease in temperature between 8 and 6.2 Ma reflects an increase in basin elevation. Because we lack other samples in this age range to confirm the warm temperature, it is also possible that the 38°C sample reflects local temperature variability due to differences in vegetative shading, topographic aspect, or other factors.

The absolute temperatures are a function of both climate and elevation, but the difference in temperature between the Puna Plateau and Eastern Cordillera samples should primarily reflect elevation, provided the temperature lapse rate when the samples were deposited was similar to today's. Atmospheric lapse rates in the lower few kilometers of the troposphere are predominantly influenced by latitude and the moisture content of the atmosphere [e.g., *Schneider*, 2007]. South America has not drifted significantly in latitude during the Cenozoic, and isotopic and geologic evidence show that the study area has been arid to semiarid since the Mid-Miocene and likely much earlier, suggesting long-term stability of atmospheric lapse rates in the study area over this interval

General circulation model experiments have suggested that climate responds nonlinearly, with significant threshold effects, to rising surface topography [*Ehlers and Poulsen*, 2009; *Insel et al.*, 2012; *Poulsen et al.*, 2010]. However, our record indicates no significant change in environmental conditions over the past 10 Ma. Also, the Puna Plateau is shown to have been at high elevations (similar to modern) since at least ~36 Ma [*Canavan et al.*, 2014]; therefore, variations in lapse rates due to changes in elevation should not be an issue [*Ehlers and Poulsen*, 2009].

Given these observations, we examine the difference in average temperatures recorded by the Puna Plateau samples collected at elevations of ~3.6 to 4.0 km and Eastern Cordillera samples collected 1.9 km lower at elevations of ~1.8 to 2.1 km. Dividing the modern difference in summer air temperature between these areas of 11.5°C by their elevation difference of 1.9 km yields a summer temperature lapse rate of approximately 6°C/km. Assuming no significant changes in climate and elevation in the area, we would expect the offset in temperature between the Angastaco basin and Puna Plateau nodules to be around 11.5°C. A two-sample *t* test indicates that the difference in the mean $T(\Delta_{47})$ values of the Angastaco basin (6.2 to 3.2 Ma samples) and Puna Plateau sample suites is 8 ± 5°C (2 σ) (*t* test, H = 1; $p = 0.0067$; d.f. = 10). Although the data permit significant change in relative elevation of the two surfaces (±0.8 km (2 σ), assuming the modern temperature lapse rate applies), the difference in mean $T(\Delta_{47})$ values is within 2σ of the expected temperature difference based on modern climate and elevation. The lack of significant temperature change through time for the two-sample suites suggests similar paleotopographic gradient and temperatures as today and, by extension, similar elevations as today.

The clumped isotope temperatures thus suggest that modern elevations were reached in the Puna Plateau (within ~ 0.3 km) by 10 Ma and in the Eastern Cordillera (within ~ 0.5 km) by 6 Ma. The δ^2H_{glass} values of volcanic ashes from the Puna Plateau and Eastern Cordillera indicate values similar to present and by inference elevations similar to modern since 10 Ma and to 7 Ma, respectively (Figure 2).

High elevations similar to modern recorded by the Eastern Cordillera glass samples from tuffs by 14 Ma are consistent with the deformation history of the region. The Angastaco basin was the site of wedge-top deposition between 14 Ma and 4 Ma [*Carrapa et al.*, 2012], and evidence of syndepositional deformation is

present at the west margin of the Angastaco basin and in the Quebrada del Toro [*DeCelles et al.*, 2011] between 14 and 11 Ma. Deformation in the Angastaco area continued until ~4 Ma as recorded by folding of Pliocene strata and low-temperature thermochronological data indicating Pliocene basin exhumation [*Carrapa et al.*, 2011]. Although the La Viña section to the east of the Angastaco basin was in a foreland basin position, it was hydrologically connected to the Angasatco basin; therefore, sample LVT1-006 is interpreted to record average elevation of the Eastern Cordillera since 14 Ma. This evidence combined with the fact that the Angastaco area was in a proximal foredeep position until 14 Ma and was in a wedge-top position between ~14 and 4 Ma [*Carrapa et al.*, 2012; *DeCelles et al.*, 2011] limit the timing of uplift of the Eastern Cordillera to between ~14 Ma and 4 Ma. Our data help better constrain the timing of uplift, indicating that the Angastaco area was at elevations similar to modern since at least 7–6 Ma and possibly as early as 14 Ma based on δ^2H values and as early as 10 Ma based on the relative difference in isotopic values between the Puna and Eastern Cordillera. Assuming an average foreland basin elevation of 400 m (Figure 2c) and an average final elevation of 1.9 km, the magnitude of uplift is estimated to be 1.5 km. We note that a 1.7 km magnitude of uplift results from assuming a 200 m foreland basin elevation. The timing of this deformation suggests that surface uplift of the Eastern Cordillera occurred during active shortening and orogenic growth.

We suggest that the Miocene concentration of long-lived deformation and surface uplift in the Eastern Cordillera reflects active shortening and crustal thickening in the region. The predicted uplift of the Eastern Cordillera, assuming that all the shortening and crustal thickening occurred in the Miocene and isostatic balance, is calculated to be 2.1 km (Figure 4). This value of predicted uplift is obtained by performing an area balance calculation assuming airy isostasy, using values of 25% shortening (from an initial undeformed length of the Eastern Cordillera of 275 km and a final shortened length of 205 km from *Grier et al.* [1991]), an original crustal thickness of 40 km (based on modern crustal thickness under the present foreland from *Beck and Zandt* [2002]), and crust and mantle density of 2.8 and 3.3 g/cm^3, respectively. The calculated uplift is consistent with the 1.5–1.7 km of uplift obtained by combining our paleoelevation proxies with independent geological evidence.

Miocene-Pliocene small-scale lithospheric foundering has been suggested under the Puna Plateau [*Schoenbohm and Carrapa*, 2009]. If small-scale lithospheric foundering occurred, our data indicate that the amount of uplift resulting from isostatic rebound following foundering must be small enough ($<$0.5–1 km) to not be detected by our techniques. This is consistent with geochemical data and geodynamic modeling showing small volume lithospheric removals under the plateau and isostatic rebound being limited to $<$1 km [e.g., *Krystopowicz and Currie*, 2013]. Geochemical and geophysical data [e.g., *Ducea et al.*, 2013; *Bianchi et al.*, 2013] also support small-scale lithospheric foundering under the Puna Plateau.

8. Conclusions

Our multiproxy paleoaltimetry analysis from the Puna Plateau and Eastern Cordillera places a temporal constraint on surface uplift of the region. The Eastern Cordillera achieved environmental conditions and elevations similar to modern between 14 Ma and 10 Ma (Figure 4). High elevation and sustained aridity in the Puna Plateau were established by 10 Ma. Clumped isotope data indicate that temperatures in the Puna Plateau and in the Eastern Cordillera were similar to modern since ~10 and ~6 Ma, respectively, and that the difference in mid-Miocene-Pliocene temperatures for the two regions is consistent with the difference in temperature and elevation of the two regions today. Our data when combined with previous geological evidence support a pre-Miocene uplift history of the Puna Plateau ($>$10 Ma) and indicate that the Eastern Cordillera experienced ~1.5 to 1.7 km of surface uplift as early as 14 Ma and by 7–6 Ma. The timing of uplift correlates with the timing of active upper crustal shortening in the region (Figure 4a).

Our study suggests that attainment of high elevation in the Eastern Cordillera of NW Argentina, and possibly the Puna Plateau, was the result of shortening and crustal thickening. We conclude that high elevations in NW Argentina were achieved during crustal thickening preceding possible lithospheric removal rather than being the result of isostatic rebound following lithospheric removal. Our data show a different uplift scenario for the Puna Plateau when compared with data from the Altiplano and Eastern Cordillera of Bolivia and suggest along-strike variability in timing and mechanisms of uplift in the Central Andes.

Acknowledgments
Funding for this research was provided by NSF EAR-0911577 to B.C. and EAR-1252064 to K.W.H. We thank Ricardo Alonso for logistical support, Laura Vietta for help in the field, and Bodo Bookhagen for help with MODIS data. We thank John Eiler for generous laboratory support.

References

Affek, H. P., X. Xu, and J. M. Eiler (2007), Seasonal and diurnal variations of $^{13}C^{18}O^{16}O$ in air: Initial observations from Pasadena, CA, *Geochim. Cosmochim. Acta*, *71*, 5033–5043.

Allmendinger, R., T. Jordan, S. Kay, and B. Isacks (1997), The evolution of the Altiplano-Puna Plateau of the Central Andes, *Annu. Rev. Earth Planet. Sci.*, *25*, 139–174.

Alonso, R., B. Carrapa, I. Coutand, M. Haschke, G. Hilley, L. M. Schoenbohm, E. R. Sobel, M. R. Strecker, and M. Trauth (2007), Tectonics, climate, and landscape evolution of the southern Central Andes: The Argentine Puna Plateau and adjacent regions between 22° and 28°S lat., in *The Andes-Active Subduction Orogeny: Frontiers in Earth Sciences*, *Monogr. Ser.*, vol. 1, edited by O. Oncken et al., pp. 265–283, Springer, Berlin.

Beck, S. L., and G. Zandt (2002), The nature of orogenic crust in the central Andes, *J. Geophys. Res.*, *107*(B10), 2230, doi:10.1029/2000JB000124.

Bershaw, J., C. N. Garzione, P. Higgins, B. J. MacFadden, F. Anaya, and H. Alvarenga (2010), Spatial–temporal changes in Andean plateau climate and elevation from stable isotopes of mammal teeth, *Earth Planet. Sci. Lett.*, *289*, 530–538.

Bianchi, M., et al. (2013), Telesesimic tomography of the southern Puna Plateau in Argentina and adjacent regions, *Tectonophysics*, *586*, 65–83.

Blisniuk, P. M., and L. A. Stern (2005), Stable isotope paleoaltimetry: A critical review, *Am. J. Sci.*, *305*, 1033–1074.

Bookhagen, B., and M. R. Strecker (2012), Spatiotemporal trends in erosion rates across a pronounced rainfall gradient: Examples from the southern Central Andes, *Earth Planet. Sci. Lett.*, *327–328*, 97–110.

Bookhagen, B., K. R. Haselton, and M. H. Trauth (2001), Hydrological modelling of a Pleistocene landslide-dammed lake in the Santa Maria Basin, NW Argentina, *Palaeogeogr. Palaeoclimatol. Palaeoecol.*, *169*, 113–127.

Breecker, D. O., Z. D. Sharp, and L. D. McFadden (2009), Atmospheric CO_2 concentrations during ancient greenhouse climates were similar to those predicted for A.D. 2100, *Proc. Natl. Acad. Sci. U. S. A.*, *107*, 576–580.

Bywater-Reyes, S. (2009), Tectonic and climatic evolution of the Angastaco Basin (25°–26°S, Eastern Cordillera, NW Argentina), MS Thesis, 142 pp., University of Wyoming.

Bywater-Reyes, S., B. Carrapa, M. Clementz, and L. Schoenbohm (2010), Effect of late Cenozoic aridification on sedimentation in the Eastern Cordillera of northwest Argentina (Angastaco basin), *Geology*, *38*, 235–238.

Canavan, R. (2010), Cenozoic paleoelevation reconstructions of the Puna Plateau, NW Argentina, MS thesis, 117 pp., Dep. of Geol. and Geophys., Univ. of Wyoming, Laramie.

Canavan, R. (2012), Cenozoic paleoelevation reconstructions of the Puna Plateau, NW Argentina, Master Thesis, 117 pp., University of Wyoming.

Canavan, R., B. Carrapa, M. Clementz, J. Quade, P. G. DeCelles, and L. Schoenbohm (2014), Early Cenozoic uplift of the Puna Plateau, Central Andes, based on stable isotope paleoaltimetry of hydrated volcanic glass, *Geology*, *42*, 447–450, doi:10.1130/G35239.1.

Carrapa, B., and P. G. DeCelles (2008), Eocene exhumation and basin development in the Puna of northwestern Argentina, *Tectonics*, *27*, TC1015, doi:10.1029/2007TC002127.

Carrapa, B., D. Adelmann, G. E. Hilley, E. Mortimer, E. Sobel, and M. R. Strecker (2005), Oligocene range uplift and development of plateau morphology in the southern central Andes, *Tectonics*, *24*, TC4011, doi:10.1029/2004TC001762.

Carrapa, B., P. G. DeCelles, P. W. Reiners, G. E. Gehrels, and M. Sudo (2009), Apatite triple dating and white mica $^{40}Ar/^{39}Ar$ thermochronology of syntectonic detritus in the Central Andes: A multiphase tectonothermal history, *Geology*, *37*, 407–410.

Carrapa, B., J. D. Trimble, and D. F. Stockli (2011), Patterns and timing of exhumation and deformation in the Eastern Cordillera of NW Argentina revealed by (U-Th)/He thermochronology, *Tectonics*, *30*, TC3003, doi:10.1029/2010TC002707.

Carrapa, B., S. Bywater-Reyes, P. G. DeCelles, E. Mortimer, and G. Gehrels (2012), Late Eocene–Pliocene basin evolution in the Eastern Cordillera of northwestern Argentina (25°–26°S): Regional implications for Andean orogenic wedge development, *Basin Res.*, *23*, 1–20, doi:10.1111/j.1365-2117.2011.00519.x.

Cassel, E. J., S. A. Graham, and C. P. Chamberlain (2009), Cenozoic tectonic and topographic evolution of the northern Sierra Nevada, California, through stable isotope paleoaltimetry in volcanic glass, *Geology*, *37*, 547–550.

Cerling, T. E. (1984), The stable isotopic composition of modern soil carbonate and its relationship to climate, *Earth Planet. Sci. Lett.*, *71*, 229–240.

Cerling, T. E., and J. Quade (1993), Stable carbon and oxygen isotopes in soil carbonates, in *Continental Indicators of Climate, Proceedings of Chapman Conference, Jackson Hole, Wyoming*, *Monogr.*, vol. 78, edited by P. Swart, J. A. McKenzie, and K. C. Lohman, pp. 217–231, AGU, Washington, D. C.

Coutand, I., P. R. Cobbold, M. de Urreiztieta, P. Gautier, A. Chauvin, D. Gapais, E. A. Rossello, and O. Lòpez-Gamundí (2001), Style and history of Andean deformation, Puna Plateau, Northwestern Argentina, *Tectonics*, *20*, 210–234, doi:10.1029/2000TC900031.

Coutand, I., B. Carrapa, A. Deeken, A. K. Schmitt, E. R. Sobel, and M. R. Strecker (2006), Orogenic plateau formation and lateral growth of compressional basins and ranges: Insights from sandstone petrography and detrital apatite fission-track thermochronology in the Angastaco Basin, NW Argentina, *Basin Res.*, *18*, 1–26.

Craig, H. (1961), Isotopic Variations in Meteoric Waters, *Science*, *133*, 1702–1703, doi:10.1126/science.133.3465.1702.

Craig, H., and L. I. Gordon (1965), Deuterium and oxygen-18 variations in ocean and the marine atmosphere, in *Proceedings Stable Isotopes in Oceanographic Studies and Paleotemperatures*, pp. 277–374, Univ. of Rhode Island Press, Rhode Island.

Cristallini, E. O., A. Cominguez, and V. Ramos (1997), Deep structure of the Metan-Guachipas region: Tectonic inversion in northwestern Argentina, *J. South Am. Earth Sci.*, *10*, 403–421.

Cristallini, E. O., A. Cominguez, V. A. Ramos, and E. D. Mercerat (2004), Basement double-wedge thrusting in the northern Sierras Pampeanas of Argentina (27°S)—Constraints from deep seismic reflection, in *Thrust Tectonics and Hydrocarbon Systems*, edited by K. R. McClay, *Am. Assoc. Pet. Geol. Mem.*, *82*, 65–90.

Dansgaard, W. (1964), Stable isotopes in precipitation, *Tellus*, *16*, 436–468.

DeCelles, P. G., M. Ducea, G. Zandt, and P. Kapp (2009), Cyclicity in Cordilleran orogenic systems, *Nature*, *2*, 251–257.

DeCelles, P. G., B. Carrapa, B. Horton, and G. Gehrels (2011), Cenozoic foreland basin system in the central Andes of northwestern Argentina: Implications for Andean geodynamics and modes of deformation, *Tectonics*, *30*, TC6013, doi:10.1029/2011TC002948.

Deeken, A., E. R. Sobel, I. Coutand, M. Haschke, U. Riller, and M. R. Strecker (2006), Construction of the southern Eastern Cordillera, NW Argentina: From early Cretaceous extension to middle Miocene shortening, constrained by AFT-thermochronometry, *Tectonics*, *25*, TC6003, doi:10.1029/2005TC001894.

Dennis, K. J., H. P. Affek, B. H. Passey, D. P. Schrag, and J. M. Eiler (2011), Defining an absolute reference frame for 'clumped' isotope studies of CO_2, *Geochim. Cosmochim. Acta*, *75*, 7117–7131.

Dettinger, M. P. (2012), Calibrating and testing the volcanic glass paleoaltimeter in South America, MS thesis, 53 pp., University of Arizona.

Ducea, M. N., A. C. Seclaman, K. E. Murray, D. Jianu, and L. M. Schoenbohm (2013), Mantle-drip magmatism beneath the Altiplano-Puna Plateau, central Andes, *Geology*, *41*, 915–918.

Ehlers, T., and C. J. Poulsen (2009), Influence of Andean uplift on climate and paleoaltimetry estimates, *Earth Planet. Sci. Lett.*, *281*, 238–248.
Eiler, J. M. (2007), Clumped-isotopegeochemistry—The study of naturally-occurring, multiply-substituted isotopologues, *Earth Planet. Sci. Lett.*, *262*, 309–327.
Eiler, J. M. (2011), Paleoclimate reconstructions using carbonate clumped isotope thermometry, *Quat. Sci. Rev.*, *30*, 3575–3588.
Eiler, J. M., and E. Schauble (2004), $^{18}O^{13}C^{16}O$ in Earth's atmosphere, *Geochim. Cosmochim. Acta*, *68*, 4767–4777.
Eiler, J. M., C. N. Garzione, and P. Ghosh (2006), Response to Comments on "Rapid uplift of the Altiplano revealed through $^{13}C\backslash^{18}O$ bonds in paleosol carbonates", *Science*, *314*, 760.
Fan, M. J., P. G. DeCelles, G. E. Gehrels, D. L. Dettman, J. Quade, and S. L. Peyton (2011), Sedimentology, detrital zircon geochronology, and stable isotope geochemistry of the lower Eocene strata in the Wind River Basin, central Wyoming, *Geol. Soc. Am. Bull.*, *123*, 979–996.
Fox, D. L., and P. L. Koch (2004), Carbon and oxygen isotopic variability in neogene paleosol carbonates: Constraints on the evolution of the C^{40}grasslands of the Great Plains, USA, *Palaeogeogr. Palaeoclimatol. Palaeoecol.*, *207*, 305–329.
Friedman, I., J. Gleason, R. A. Sheppard, and A. J. Gude (1993), Deuterium fractionation as water diffuses into silicic volcanic ash, in *Continental Indicators of Climate, Proceedings of Chapman Conference, Jackson Hole, Wyoming*, *Monogr.*, vol. 78, edited by P. Swart, J. A. McKenzie, and K. C. Lohman, pp. 321–323, AGU, Washington, D. C.
Garzione, C. N., P. Molnar, J. C. Libarkin, and B. J. MacFadden (2006), Rapid late Miocene rise of the Bolivian Altiplano: Evidence for removal of mantle lithosphere, *Earth Planet. Sci. Lett.*, *241*, 543–556.
Garzione, C., G. D. Hoke, J. C. Libarkin, S. Withers, B. MacFadden, J. Eiler, P. Ghosh, and A. Mulch (2008), The Rise of the Andes, *Science*, *320*, 1304, doi:10.1126/science.1148615.
Garzione, C. N., D. J. Auerbach, J. Jin-SookSmith, J. J. Rosario, B. H. Passey, T. E. Jordan, and J. M. Eiler (2014), Clumped isotope evidence for diachronous surface cooling of the Altiplano and pulsed surface uplift of the Central Andes, *Earth Planet. Sci. Lett.*, *393*, 173–181.
Gazis, C., and X. Feng (2004), A stable isotope study of soil water: Evidence for mixing and preferential flow paths, *Geoderma*, *119*, 97–111.
Ghosh, P., J. Adkins, H. Affek, B. Balta, W. Guo, E. A. Schauble, D. Schrag, and J. M. Eiler (2006a), $^{13}C–^{18}O$ bonds in carbonate minerals: A new kind of paleothermometer, *Geochim. Cosmochim. Acta*, *70*, 1439–1456.
Ghosh, P., C. N. Garzione, and J. M. Eiler (2006b), Rapid uplift of the Altiplano revealed in abundances of $^{13}C—^{18}O$ bonds in paleosol carbonate, *Science*, *311*, 511–515.
Godfrey, L. V., T. E. Jordan, T. K. Lowenstein, and R. L. Alonso (2003), Stable isotope constraints on the transport of water to the Andes between 22 degrees and 26 degrees S during the last glacial cycle, *Palaeogeogr. Palaeoclimatol. Palaeoecol.*, *194*(1–3), 299–317, doi:10.1016/S0031-0182(03)00283-9.
Gregory-Wodzicki, K. M. (2000), Uplift history of the Central and Northern Andes: A review, *Geol. Soc. Am. Bull.*, *112*(7), 1091–1105.
Grier, M., J. Salfity, and R. Allmendinger (1991), Andean reactivation of the Cretaceous Salta rift, northwestern Argentina, *J. South Am. Earth Sci.*, *4*, 351–372.
Guo, W., and J. M. Eiler (2007), Temperatures of aqueous alteration and evidence for methane generation on the parent bodies of the CM Chondrites, *Geochim. Cosmochim. Acta*, *71*, 5565–5575.
Haschke, M., W. Siebel, A. Günter, and E. Scheuber (2002), Repeated crustal thickening and recycling during the Andean orogeny in north Chile (21°S–26°S), *J. Geophys. Res.*, *107*(B1), 2019, doi:10.1029/2001JB000328.
Henderson, A. K., and B. Shuman (2009), Hydrogen and oxygen isotopic composition of lake-water in the western U.S., *Geol. Soc. Am. Bull.*, *121*, 1179–1189, doi:10.1130/B26441.1.
Henkes, G. A., B. H. Passey, E. L. Grossman, A. Perez-Huera, B. Shenton, and T. E. Yncey (2014), The temperature limits for preservation of primary calcite clumped isotope paleotemperatures, *Geochim. Cosmochim. Acta*, doi:10.1016/j.gca.2014.04.040.
Hillel, D. (1982), *Introduction to Soil Physics*, Academic Press, San Diego, Calif.
Hoke, G. D., and C. N. Garzione (2008), Paleosurfaces, paleoelevation, and the mechanisms for the late Miocene topographic development of the Altiplano plateau, *Earth Planet. Sci. Lett.*, *271*, 192–201.
Hren, M. T., and N. D. Sheldon (2012), Temporal variations in lake water temperature: Paleoenvironmental implications of lake carbonate $\delta^{18}O$ and temperature records, *Earth Planet. Sci. Lett.*, *337*, 77–84, doi:10.1016/j.epsl.2012.05.019.
Hsieh, J. C. C., O. A. Chadwick, E. F. Kelly, and S. M. Savin (1998), Oxygen isotopic composition of soil water: Quantifying evaporation and transpiration, *Geoderma*, *82*, 269–293.
Huntington, K. W., et al. (2009), Methods and limitations of 'clumped' CO2 isotope (D47) analysis by gas-source isotope ratio mass spectrometry, *J. Mass Spectrom.*, *44*, 1318–1329, doi:10.1002/jms.1614.
Huntington, K. W., B. P. Wernicke, and J. M. Eiler (2010), Influence of climate change and uplift on Colorado Plateau paleotemperatures from carbonate clumped isotope thermometry, *Tectonics*, *29*, TC3005, doi:10.1029/2009TC002449.
IAEA/WMO (2014), Global network of isotopes in precipitation, The GNIP Database. [Available at http://www.iaea.org/water.]
Insel, N., C. J. Poulsen, T. A. Ehlers, and C. Sturm (2012), Response of meteoric $\delta^{18}O$ to surface uplift—Implications for Cenozoic Andean Plateau growth, *Earth Planet. Sci. Lett.*, *317–318*, 262–272.
Insel, N., C. J. Poulsen, C. Sturm, and T. A. Ehlers (2013), Climate controls on Andean precipitation $\delta^{18}O$ interannual variability, *J. Geophys. Res. Atmos.*, *118*, 9721–9742, doi:10.1002/jgrd.50619.
Jordan, T. E., P. Nester, N. Blanco, G. D. Hoke, F. Dávila, and A. J. Tomlinson (2010), Uplift of the Altiplano-Puna Plateau: A view from the west, *Tectonics*, *29*, TC5007, doi:10.1029/2010TC002661.
Kim, S.-T., and J. R. O'Neil (1997), Equilibrium and non-equilibrium oxygen isotope effects in synthetic carbonates, *Geochim. Cosmochim. Acta*, *61*, 3461–3475.
Kley, J., and C. R. Monaldi (1998), Tectonic shortening and crustal thickness in the Central Andes: How good is the correlation?, *Geology*, *26*, 723–726.
Kraemer, B., D. Adelmann, M. Alten, W. Schnurr, K. Erpenstein, E. Kiefer, P. van den Bogaard, and K. Görler (1999), Incorporation of the Paleogene foreland into Neogene Puna Plateau: The Salar de Antofolla, NW Argentina, *J. South Am. Earth Sci.*, *12*, 157–182.
Krystopowicz, N. J., and C. A. Currie (2013), Crustal eclogitization and lithosphere delamination in orogens, *Earth Planet. Sci. Lett.*, *361*, 195–207.
Lechler, A. R., N. A. Niemi, M. T. Hren, and K. C. Lohmann (2013), Paleoelevation estimates for the northern and central proto–Basin and Range from carbonate clumped isotope thermometry, *Tectonics*, *32*, 295–316, doi:10.1002/tect.20016.
Leier, A., N. McQuarrie, C. Garzione, and J. Eiler (2013), Stable isotope evidence for multiple pulses of rapid surface uplift in the Central Andes, Bolivia, *Earth Planet. Sci. Lett.*, *371–372*, 49–58.
Liu, B., F. M. Phillips, and A. R. Campbell (1996), Stable carbon and oxygen isotopes of pedogenic carbonates, Ajo Mountains, southern Arizona: Implications for paleoenvironmental change, *Palaeogeogr. Palaeoclimatol. Palaeoecol.*, *124*, 233–246.
Melnick, D., and H. P. Echtler (2006), Inversion of fore-arc basins in south-central Chile caused by rapid glacial age trench fill, *Geology*, *34*, 709–712.

Molnar, P., and C. N. Garzione (2007), Bounds on the viscosity coefficient of continental lithosphere from removal of mantle lithosphere beneath the Altiplano and Eastern Cordillera, *Tectonics*, *26*, TC2013, doi:10.1029/2006TC001964.

Mon, R., and J. A. Salfity (1995), Tectonic evolution of the Andes of northern Argentina, in *Petroleum Basins of South America*, edited by A. J. Tankard, R. S. Soruco, and H. J. Welsink, *Am. Assoc. Pet. Geol. Mem.*, *62*, 269–283.

Passey, B. H., and G. A. Henkes (2012), Carbonate clumped isotope bond reordering and geospeedometry, *Earth Planet. Sci. Lett.*, *351–352*, 223–236.

Passey, B. H., N. E. Levin, T. E. Cerling, F. H. Brown, and J. M. Eiler (2010), High temperature environments of human evolution in East Africa based on bond ordering in paleosol carbonates, *Proc. Natl. Acad. Sci. U. S. A.*, *107*, 11,245–11,249.

Peters, N. A., K. Huntington, and G. D. Hoke (2013), Hot or not? Impact of seasonally variable soil carbonate formation on paleotermperature and O-isotope records from clumped isotope thermometry, *Earth Planet. Sci. Lett.*, *361*, 208–218.

Poage, M., and P. C. Chamberlain (2001), Empirical relationships between elevation and the stable isotope composition of precipitation and source waters: Considerations for studies of paleoelevation change, *Am. J. Sci.*, *301*, 1–15.

Poulsen, C. J., and M. L. Jeffery (2011), Climate change imprinting on stable isotopic compositions of high-elevation meteoric water cloaks past surface elevations of major orogens, *Geology*, *39*(6), 595–598.

Poulsen, C. J., T. Ehlers, and N. Insel (2010), Onset of convective rainfall during gradual late Miocene rise of the central Andes, *Science*, *328*, 490–493.

Quade, J., C. Garzione, and J. Eiler (2007), Paleoelevation reconstruction using pedogenic carbonates, *Rev. Mineral. Geochem.*, *66*, 53–87.

Quade, J., D. O. Breecker, M. Daeron, and J. Eiler (2011), The paleoaltimetry of Tibetan isotopic perspective, *Am. J. Sci.*, *311*, 77–115.

Quade, J., J. Eiler, M. Daëron, and H. Achuythan (2013), The clumped isotope paleothermometer in soils and paleosol carbonate, *Geochim. Cosmochim. Acta*, *105*, 92–107.

Rowley, D., and C. Garzione (2007), Stable isotope-based paleoaltimetry, *Annu. Rev. Earth Planet. Sci.*, *35*, 463–508.

Saylor, J. E., J. Quade, D. L. Dettman, P. G. DeCelles, P. A. Kapp, and L. Ding (2009), The late Miocene through present paleoelevetation history of southwestern Tibet, *Am. J. Sci.*, *309*, 1–42, doi:10.2475/01.2009.01.

Schneider, T. (2007), Thermal stratification of the extratropical troposphere, in *The Global Circulation of the Atmosphere*, edited by T. Schneider and A. H. Sobel, pp. 47–77, Princeton Univ. Press, Princeton, N. J.

Schoenbohm, L., and B. Carrapa (2009), Structural evidence for lithospheric foundering in the Puna Plateau, NW Argentina, *Eos Trans. AGU*, *89*(1), Spring Meet. Suppl., Abstract T12A-01.

Sempere, T., A. Hartley, and P. Roperch (2006), Comment on "Rapid uplift of the Altiplano revealed through ^{13}C–^{18}O bonds in paleosol carbonates", *Science*, *314*, 760, doi:10.1126/science.1132837.

Sewall, J. O., and H. C. Fricke (2013), Andean-scale highlands in the Late Cretaceous Cordillera of the North American western margin, *Earth Planet. Sci. Lett.*, *362*, 88–98.

Snell, K. E., B. L. Thrasher, J. M. Eiler, P. L. Koch, L. C. Sloan, and N. J. Tabor (2013), Hot summers in the Bighorn Basin during the early Paleogene, *Geology*, *41*, 55–58.

Starck, D., and L. M. Anzotegui (2001), The late Miocene climatic change-persistance of a climatic signal through the orogenic stratigraphic record in northwestern Argentina, *J. South Am. Earth Sci.*, *14*, 763–774.

Strecker, M., R. Alonso, B. Bookhagen, B. Carrapa, G. Hilley, E. Sobel, and M. Trauth (2007), Tectonics and climate of the southern central Andes, *Annu. Rev. Earth Planet. Sci.*, *35*, 747–787.

Vandervoort, D. S., T. E. Jordan, P. K. Zeitler, and R. N. Alonso (1995), Chronology of internal drainage development and uplift, southern Puna Plateau, Argentine Central Andes, *Geology*, *23*, 145–148.

Vuille, M., and M. Warner (2005), Stable isotopes in precipitation recording South American summer monsoon and ENSO variability: Observations and model results, *Clim. Dyn.*, *25*, 401–413, doi:10.1007/s00382-005-0049-9.

Wan, Z., P. Wang, and X. Li (2004), Using MODIS land surface temperature and normalized difference vegetation index products for monitoring drought in the southern Great Plains, USA, *Int. J. Remote Sens.*, *25*, 61–72.